

Global/Local FEM-BEM Stress Analysis of Damaged Aircraft Structures

A. Alaimo¹, A. Milazzo² and C. Orlando³

Abstract: In this paper a Hierarchical approach for the analysis of advanced aerospace structures is presented. The proposed Global/Local model uses two kind of numerical methods. The first step of the Hierarchical procedure is performed by the Finite Element code Patran/NastranTM, using a coarse mesh to study the global structure, then the local region is analyzed by using a Boundary Element code based on the multidomain anisotropic technique. This code accurately predicts stress concentrations at crack tips with a reduction of the modeling efforts and of the computational time. The Global/Local interface code implemented allows an intuitive extraction of the local region with a substantial reduction of the modeling time. The accuracy and the effectiveness of the model have been demonstrated analyzing classical stress concentration problems. Then the procedure has been used to analyze more complex structures among which a riveted patch repair, applied on a cracked panel, and a cracked graphite-epoxy curved panel with Z stiffeners and Z frames.

Keyword: Global/Local, Hierarchical, Boundary Element Method, Finite Element Method, Stress Intensity Factor.

1 Introduction

The field of aeronautical and aerospace structures has seen the rapid growth of the use of composite materials. Their inherent features make them very suitable in the framework of reliable lightweight structures. The high stiffness to weight and strength to weight ratio of these materials as well as the path-loads management

¹ Dipartimento di Tecnologie ed Infrastrutture Aeronautiche, University of Palermo, Palermo, Italy, e-mail: a.alaimo@unipa.it.

² Dipartimento di Tecnologie ed Infrastrutture Aeronautiche, University of Palermo, Palermo, Italy, e-mail: alberto.milazzo@unipa.it.

³ Dipartimento di Tecnologie ed Infrastrutture Aeronautiche, University of Palermo, Palermo, Italy, e-mail: c.orlando@unipa.it.

capability allow remarkable structural weight savings with linked engineering, economic and pollution reduction gains, see Noor (2000). These considerations as well as advancing and maturing of manufacturing technologies, see Ngo (2004), has driven the aerospace industry and market to consider the feasibility of all-composite small size business aircraft and of the construction of medium and large size civil aircraft with all-composite pressurized fuselages. Very remarkable examples of this trend are given by the design of the Airbus A380, see Dornheim (2001), and Boeing 787, see King (2007). The reason of this increasing interest is especially based on the advantage of a reduced overall structural complexity, accomplished through the manufacturing of large size panels with less riveted joints. This leads to low parts count and consequently to a decreasing of the stress concentration points, to easy maintenance and to the overall reduction of manufacturing and inspection times and costs. Anyway, although the emerging trend of the aeronautical field is developing along the aforementioned paths, extreme caution must be devoted to the employment of composite materials in highly loaded structures and to the evaluation of the reliability of the allowed new configurations. The behavior of these structures, in particular if cutouts, holes or cracks are present, appears very complex and therefore accurate and efficient numerical modeling strategies are needed to caught their structural behavior close to the discontinuities Atluri (1997). In order to reduce the computational effort required to achieve reliable solutions, the Global/Local approach has been proposed. This hierarchical technique is based on the concept that a structure is globally analyzed by using a coarse mesh with the aim to obtain appropriate boundary condition to impose in a restricted region where a much more refined mesh is applied. Moreover, since different level of analysis are requested in a G/L context, particular and appropriate solution methods can be chosen for the specific problem under study. Then for fracture mechanics problems the local analysis may be performed by the Boundary Element Method, see Shah (2006) and Forth (2005), or the Schwartz-Neumann Alternating Technique, see Nikishkov (1994). The pioneering work about this subject was published by Mote (1971). Later many strategies have been proposed for implementing Global/Local techniques including coupling of finite element and boundary element methods, see Zienkiewicz (1997) and Belyschko (1989), finite element and spectral methods, see Belyschko (1990) and finite element and finite difference methods, see Dow (1992), finite element and Schwartz-Neumann Alternating Method, see Park (1995). More recently an automated Global/Intermediate/Local technique, in which the Finite Element Alternating method is used for the local analysis, see Atluri (1995) and Pipkins (1996), was proposed by Kawai (1999). Coupling of SGBEM and FEM Alternating Method is also used for fracture mechanics problems by Nikishkov (2001) and Han (2002).

In this paper a Global/Local approach is presented. The Global analyses are performed by using a finite elements code, while a boundary element code for anisotropic media, based on a multidomain technique, see Banerjee (1981), Blandford (1981), Tan (1992) and Milazzo (2006), is used to analyze the refined local models. The displacement field, deriving from the coarser model, is used as boundary conditions to perform the subsequent level of the analysis. Moreover, when the local region includes one or more bolted joints, the pin loading are preliminary calculated during the Global analysis and then transferred, coupled with the displacement field, as boundary conditions for the local ones. It is worth noting that the possible presence of cracks and holes in the structures analyzed is only considered in the local refined model. For this purpose the multidomain BEM code shows its attitude to easier model the cracks and the holes if compared with finite elements. To show the effectiveness and the accuracy of the proposed Global/Local approach, two examples are presented. The first deals with the analysis of a riveted patch repair, applied on a cracked panel while the second concerns with the analysis of a cracked graphite-epoxy curved panel with Z stiffeners and Z Frames.

2 Procedure of the Global/Local approach

The overall solution strategy adopted in this paper is based on the inheritance concept. The behavior shown by the refined model strongly depends upon the data inherited by the global analysis performed on the coarser model. The links between the two models are the material constants, some common geometric properties and the displacements continuity along the interface. To perform an accurate Global/Local analysis three key points must be considered: (i) an adequate characterization of the coarser model; it means that particular attention must be paid in the choose of the simplified structural schema which will govern the behavior of the more refined region; (ii) the hierarchical interface problem; the inherited global data could not exactly match with the more refined mesh of the local model and so the use of an interpolation region becomes mandatory; (iii) an accurate local analysis must be carried out paying particular attention to mesh refinement close to the stress concentration areas. Fig. 1 shows a scheme of the procedure employed in this work to model complex aerospace structures like cracked curved stiffened fuselage panels. The Global analysis is performed by Patran/Nastran™ finite element code whereas the Local analysis employs a multidomain boundary element code developed by the authors for Fracture Mechanics problems. The Global analyses involve 3D shell elements to model the skin and 1D bar elements to model stringers and fasteners. At this level of analysis neither of cracks and holes are considered avoiding time consuming and difficulties associated to the finite element modeling of these stress concentration sources.

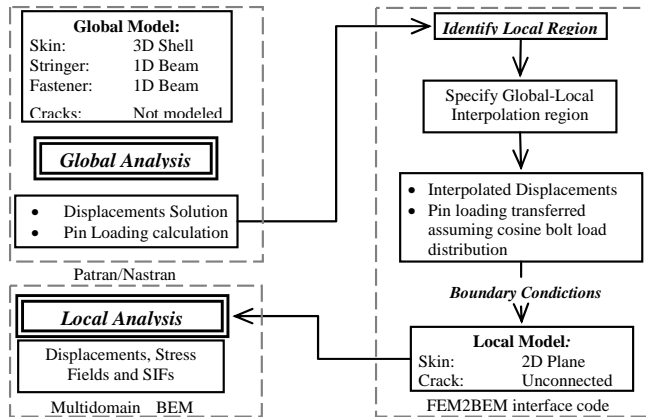


Figure 1: Global/Local scheme.

The core of the approach is the automated FEM2BEM interface code which automatically creates the local region and its mesh. It will be briefly described in the following section.

3 Global/Local Interface

The finite element modeling of the structural response in presence of stress singularities may be complex and time expensive. For this reason in the Global analyses cracks and holes are neglected. However, because the cracks and holes need to be recognized by the Global/local interface code to obtain an automatic local model generation, some techniques are developed. The cracks are located directly on the coarser model using BAR elements, see MSCSoftware (2005), having as material and property name 'CRACK', no more than a flag. It is worth noting that the 'BAR CRACK elements' are not taken into account in the FE Global analysis but they represent only dummy elements used by the interface code to recognize the presence of cracks. 1D BAR elements are also used to model the pins. Through the flag 'PIN', given as material and property name, the Global/Local Interface code is able to: (i) recognize the fastener location; (ii) create, in the Local region, holes having the same radius of the rivet; (iii) transfer to the local region the pin loading computed during the Global analysis by assuming radial stress distribution varying as a cosine function and applied over half the hole, see Waszczak (1971), DeJong (1977), Her (1998). The interface code implemented extracts all the Global model data from the text files used by Patran/Nastran™ to store information and then the Global FE model can be shown with highlighted the location of cracks and holes. The user can now choose the Local region simply by selecting an area containing

the stress concentration sources as shown in Fig. 2.

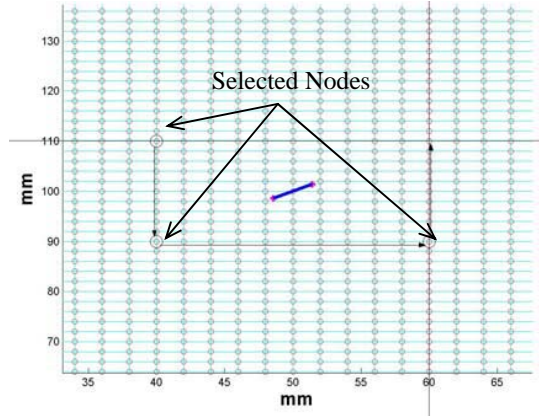


Figure 2: Extraction of the local region.

4 Local Analysis

As mentioned above, the local analyses are performed by using a BEM code based on a multidomain anisotropic technique. In this section will be briefly described the boundary element formulation developed for two-dimensional elastic domains Ω with boundary $\partial\Omega$ lying in the x_1x_2 planes, under the hypothesis of linear elasticity and plain strain field. The elastic state of the body is described in terms of mechanical displacements $\mathbf{u} = [u_1 \ u_2 \ u_3]^T$, strains $\boldsymbol{\varepsilon} = [\varepsilon_{11} \ \varepsilon_{22} \ \varepsilon_{12} \ \varepsilon_{13} \ \varepsilon_{23} \ \varepsilon_{33}]^T$ and stresses $\boldsymbol{\sigma} = [\sigma_{11} \ \sigma_{22} \ \sigma_{12} \ \sigma_{13} \ \sigma_{23} \ \sigma_{33}]^T$. The compatibility relationships, the elastic equilibrium equations and the Hooke's law, may be expressed in matrix form as follows, see Davi (2001)

$$\boldsymbol{\varepsilon} = D\mathbf{u}, \quad D^T\boldsymbol{\sigma} + \mathbf{f} = \mathbf{0}, \quad \boldsymbol{\sigma} = \mathbf{E}\boldsymbol{\varepsilon} \quad (1)$$

where \mathbf{f} is the body force vector, \mathbf{E} is the elasticity matrix and the differential operator D is defined as in Davi (2001). By combining the Eqs.1, the governing equations, completed by considering the essential and natural boundary conditions, are obtained

$$D^T\mathbf{E}D\mathbf{u} + \mathbf{f} = \mathbf{0} \text{ with } \begin{cases} \mathbf{u} = \bar{\mathbf{u}} & \text{on } \partial\Omega_u \\ \mathbf{t} = D_n^T\mathbf{E}D\mathbf{u} = \bar{\mathbf{t}} & \text{on } \partial\Omega_t \end{cases} \quad (2)$$

where D_n is the traction operator defined as in Davi (2001). Applying the reciprocity theorem and considering a particular displacement field, corresponding to a

concentrated force acting in an infinite domain and applied at the point P_0 , the well known Somigliana identity for elasticity in matrix form can be obtained

$$\mathbf{c}^* \mathbf{u}(P_0) + \int_{\partial\Omega} (\mathbf{t}^* \mathbf{u} - \mathbf{u}^* \mathbf{t}) d\partial\Omega = \int_{\Omega} \mathbf{u}^* \mathbf{f} d\Omega \quad (3)$$

where the matrix \mathbf{c}^* can be calculated according to Davì (1989), while \mathbf{u}^* and \mathbf{t}^* represent the fundamental solutions that can be deduced by a modified Lekhnitskii's approach, see Lekhnitskii (1963). The boundary integral formulation has been numerically implemented by using the Boundary Element Method, see Aliabadi (2002). According to the Boundary Element Method, the domain boundary $\partial\Omega$ is subdivided into m elements and the governing integral equations of the problem are therefore discretized by expressing the generalized boundary variables \mathbf{u} and \mathbf{t} in terms of the corresponding nodal values $\mathbf{\Delta}_{(k)}$ and $\mathbf{P}_{(k)}$

$$\begin{aligned} \mathbf{u} &= \mathbf{N} \mathbf{\Delta}_{(k)} \text{ on } \partial\Omega_{(k)} \\ \mathbf{t} &= \mathbf{\Psi} \mathbf{P}_{(k)} \text{ on } \partial\Omega_{(k)} \end{aligned} \quad (4)$$

where \mathbf{N} and $\mathbf{\Psi}$ are matrices of standard shape function. In the absence of body forces, the discretized version of Eq.3 for any point P_i is therefore given by

$$\mathbf{c}_i^* \mathbf{u}(P_i) + \sum_{k=1}^m \mathbf{H}_{ik} \mathbf{\Delta}_{(k)} + \sum_{k=1}^m \mathbf{G}_{ik} \mathbf{P}_{(k)} = 0 \quad (5)$$

\mathbf{H}_{ik} and \mathbf{G}_{ik} are the displacement and traction influence matrices defined as

$$\begin{aligned} \mathbf{H}_{ik} &= \int_{\partial\Omega_{(k)}} \mathbf{t}^*(P, P_i) \mathbf{N}(P) d\partial\Omega \\ \mathbf{G}_{ik} &= - \int_{\partial\Omega_{(k)}} \mathbf{u}^*(P, P_i) \mathbf{\Psi}(P) d\partial\Omega \end{aligned} \quad (6)$$

By collocating the point P_i at the boundary nodes the following linear algebraic system is obtained

$$\mathbf{H} \mathbf{\Delta} + \mathbf{G} \mathbf{P} = \mathbf{0} \quad (7)$$

Coupled with the proper boundary conditions it provides the solution of the problems in terms of nodal displacements and tractions. When the investigated domain is made up of piece-wise different materials or when cracks and/or inclusions need to be modeled the problem can be solved by using a multidomain approach, see Banerjee (1981) and Milazzo (2006).

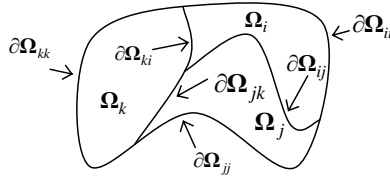
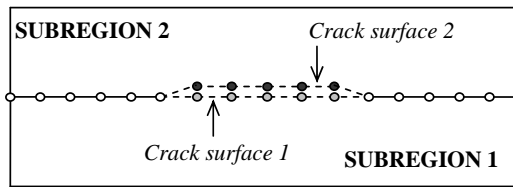


Figure 3: Multidomain Configuration.

This technique is based on the partition of the original domain into homogeneous subregions, as shown in Fig. 3, so that Eq. 5 and 7 still hold for each single subdomain. It follows that the linear algebraic system represented by Eq.7 can be written for each single subdomain

$$\mathbf{H}^{(i)} \mathbf{\Delta}^{(i)} + \mathbf{G}^{(i)} \mathbf{P}^{(i)} = \mathbf{0} (i = 1, 2, \dots, M) \quad (8)$$

where M is the number of subregions considered and the superscript (i) denotes quantities associated with the i -th subdomain. To obtain the final numerical model the domain integrity needs to be restored by enforcing the displacement continuity and traction equilibrium conditions along the interface between contiguous subdomains with the only exception for the nodes belonging the crack surfaces, as shown in Fig. 4.



- Interface coincident nodes
- Nodes belonging crack surface 1
- Nodes belonging crack surface 2

Figure 4: Multidomain crack modeling strategies.

Let us introduce a partition of the linear algebraic system given by Eq. 8 in such a

way that the generic vector $\mathbf{y}^{(i)}$ can be written as

$$\mathbf{y}^{(i)} = \begin{bmatrix} \mathbf{y}_{\partial\Omega_{i1}}^{(i)} \\ \vdots \\ \mathbf{y}_{\partial\Omega_{iM}}^{(i)} \end{bmatrix} \quad (9)$$

where the vector $\mathbf{y}_{\partial\Omega_{ij}}^{(i)}$ collects the components of $\mathbf{y}^{(i)}$ associated with the nodes belonging to the interface $\partial\Omega_{ij}$ between the i -th and j -th subdomain, assuming that $\partial\Omega_{ij}$ denotes the external boundary of the i -th sub domain, as shown in Fig. 3. In the presence of a crack, the external boundary $\partial\Omega_{ij}$ of the generic i -th subdomain also includes one of the crack surfaces in which free traction condition must be imposed. By so doing, in the discretized model the interface compatibility and equilibrium conditions, that is the interface continuity conditions, are written as

$$\Delta_{\partial\Omega_{ij}}^{(i)} = \Delta_{\partial\Omega_{ij}}^{(j)} \quad (i = 1, \dots, M-1; j = i+1, \dots, M) \quad (10)$$

$$\mathbf{P}_{\partial\Omega_{ij}}^{(i)} = -\mathbf{P}_{\partial\Omega_{ij}}^{(j)} \quad (i = 1, \dots, M-1; j = i+1, \dots, M) \quad (11)$$

If the i -th and j -th subdomain have no common boundary, $\mathbf{y}_{\partial\Omega_{ij}}^{(i)}$ is a zero-order vector and Eq. 10 and 11 are no longer valid. Eq. 8, 10 and 11 provide a set of relationship, which together with the boundary conditions on the external boundaries allows the determination of the mechanical response in terms of nodal displacements and tractions on the boundary of each subdomain.

5 Example and discussion

To demonstrate the high efficiency and versatility of the proposed Global/Local approach and to show the accuracy of the multidomain BEM code used for the analysis of the local refined models, two examples are proposed. The first concerns with the fracture mechanics analysis of a riveted patch repair applied over a fuselage skin panel. The patch consists of a single doubler applied over a cut out and a crack emanating from one of the rivet hole of the skin is considered, see Armentani (2006). The second example deals with the analysis of a cracked graphite-epoxy curved panel with Z stiffeners and Z frames. In this case the results have been compared with those obtained from a single finite element analysis in which the local refinement has been included in the global model. For simplicity this kind of analysis will be called in the following as ‘‘Global Refined FEM’’.

5.1 Example 1

The first application deals with a riveted patch repair applied over a cracked fuselage panel whose geometry, material properties and boundary condition are taken from Armentani (2006). The configuration analyzed undergoes a bi-axial stress, $\sigma_x = \sigma_y = 100$ MPa and due to symmetry only one quarter of the structure is considered as shown in Fig. 5. This configuration shows the effectiveness of the Global/Local model proposed if used for the modeling of cracked structures with cracks emanating from rivet hole.

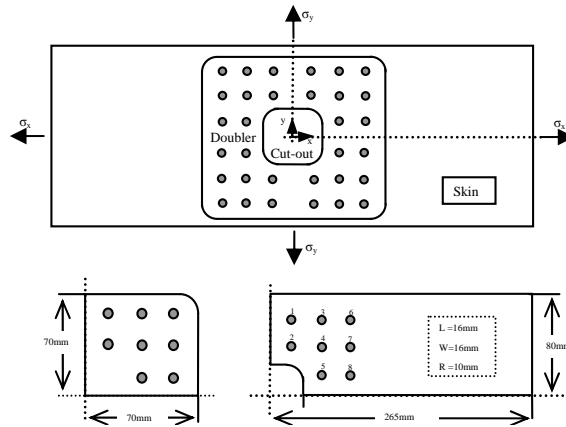


Figure 5: Geometry and Loading configuration.

5.1.1 Global Analysis

In the Global model the fasteners, connecting the doubler to the skin, are simply modeled as single bar element (see Fig. 6) having the same geometry and the same material properties as the rivets. Moreover the holes are not modeled and consequently degenerate into nodes, see AGARD (1987). In order to access the reliability of the above mentioned pin model the configuration 2, described in Tab. 1, has been analyzed and the pin loading compared with those computed by Armentani (2006). The Global analysis of configuration 2, whose computational times are equal to about 40 seconds, is based on 25867 four nodes quadrilateral elements and 8 bar elements with a total number of nodes of 21307. The pin loading and the percentage differences are listed in Tab. 2-4. It is worth noting that no modeling difficulties are associated with the construction of the global model since a simple automatic IsoMesh has been used for the analysis, see MSCSoftware (2005).

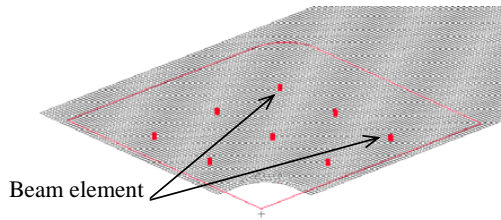


Figure 6: Doubler-Skin connection (Pin model).

Configuration 1, described in Tab. 1, has been analyzed to find the most loaded hole and the displacement field to be used as boundary condition for the local analysis performed on a restricted region surrounding the above mentioned rivet hole. The Global model and the run times for the Global analysis are the same as for configuration 2. The most loaded hole is the sixth over which a maximum pin load of 543 N acts.

Table 1: Characteristics of the two configuration analyzed

Configuration	Skin thickness (mm)	Doubler thickness (mm)	Rivet diameter (mm)	Rivet shear stiffness (N/mm)
1	1.2	1.4	4	2.9×10^4
2	1.4	1.6	4	3.1×10^4

Table 2: Pin loading Global/local, Configuration 2.

Pin	Global/Local		
	$F_x(N)$	$F_y(N)$	$F_{tot}(N)$
1	-81	-482	488
2	-107	-347	363
3	-240	-446	506
4	-268	-269	380
5	-343	-108	360
6	-422	-421	596
7	-445	-241	506
8	-476	-82	483

Table 3: Pin loading FEM Armentani (2006), Conf. 2.

Pin	FEM Armentani (2006)		
	$F_x(\text{N})$	$F_y(\text{N})$	$F_{tot}(\text{N})$
1	-83	-488	495
2	-112	-336	354
3	-242	-449	510
4	-254	-257	362
5	-326	-110	344
6	-433	-429	610
7	-444	-240	505
8	-475	-82	482

Table 4: Pin loading BEM, configuration 2.

Pin	BEM Armentani (2006)			Error(%)
	$F_x(\text{N})$	$F_y(\text{N})$	$F_{tot}(\text{N})$	(GL- FEM)/GL
1	-81	-485	492	1.4
2	-109	-334	352	2.5
3	-235	-448	506	0.8
4	-249	-256	357	4.7
5	-317	-112	336	4.4
6	-417	-430	599	2.3
7	-428	-242	492	2.8
8	-455	-87	464	0.2

5.1.2 Local Analysis

With the aim to compare the results with those obtained by Armentani (2006) two different Local analyses have been performed. The first concerns a restricted region surrounding the most loaded hole, shown in Fig. 7, in which no crack is considered. This analysis allows to choose the crack initiation site corresponding to the point in which the maximum principal stress acts. The second Local analysis is performed on the same region where a crack having length 1 mm, emanating from the point of the hole in which maximum principal stress acts, is considered. The local model, related to the local region without crack, consists of 120 constant boundary elements as shown in Fig. 7 and only few seconds are needed for the analysis. In Fig. 8 the maximum principal stresses at hole six are shown with the most loaded crack initiation site located at point A.

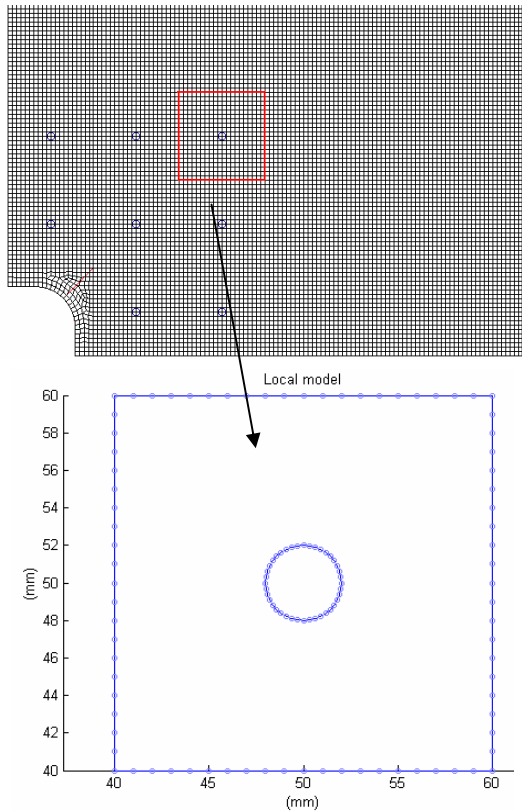


Figure 7: Mesh of the global/local region without crack.

The second Local analysis is performed on a cracked region surrounding the sixth hole. The crack emanates from point A of Fig. 8 and has a length of 1 mm. The boundary mesh, shown in Fig. 9, consists of 310 constant elements. In this case the run time is of about 25 seconds. The SIFs are computed using the crack tip opening displacements, see Aliabadi (2002). Only KI has been considered since the loading condition on the crack tip is pure Mode I. The crack is in fact oriented perpendicular to the maximum circumferential stresses. The SIF obtained by the Global/Local analysis is $KI=330 \text{ MPa mm}^{1/2}$. Comparing the above result with the SIF obtained by the non-linear iterative contact analysis performed by Armentani (2006) the percentage difference found is 1.5%.

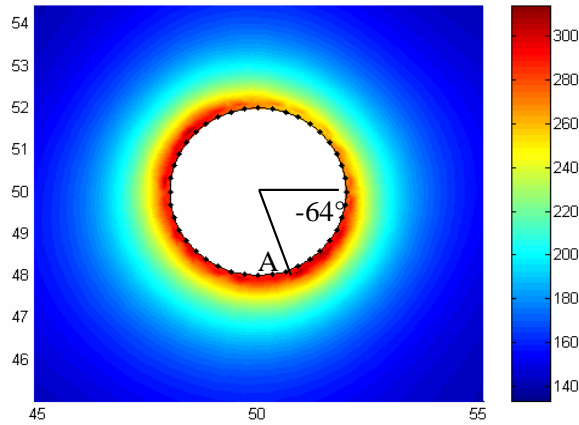


Figure 8: Maximum principal stress (MPa) at hole six.

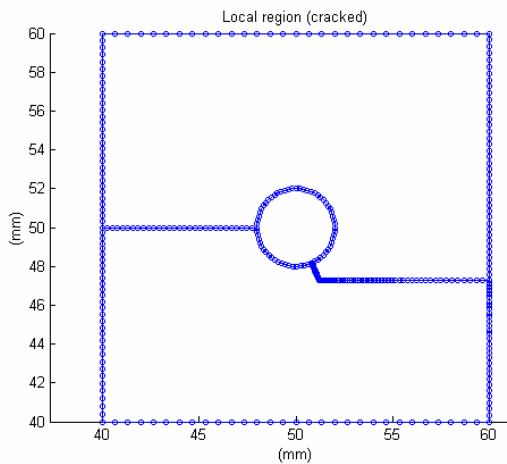


Figure 9: Mesh of the local region with crack.

5.2 Example 2

The second analysis is carried out on a curved stiffened composite panel with a longitudinal crack having length $L=27.3$ mm undergoing an internal pressure $p=55$ kPa. The geometry of the structure, shown in Fig. 10, is taken from Young (2001), while the material properties are listed in Fig. 10. This configuration is analyzed to show the efficiency and the accuracy of the Global/Local approach proposed upon a single Global Refined FEM analysis for the study of the fracture mechanics behavior of complex structure. With this purpose two different analyses have been

carried out. The first one, performed by using Patran/Nastran™, deals with a Global Refined FEM model studied in a single step, while the second analysis is performed by the Global/Local approach proposed.

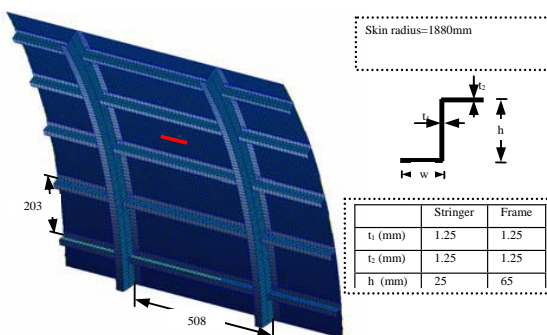


Figure 10: Geometry of the fuselage panel.

5.2.1 Global/Local analysis

The finite element Global model consists of 6400 four node quadrilateral elements used to model the skin, and of 560 two nodes beam elements used to model the stringers and the frames. Once again the global model does not introduce high modeling difficulties since at this level of analysis no singular zones need to be modeled. The time needed for the Global analysis is of about 52 seconds. Fig. 11 shows the local region extracted from the global one. The two subdomains, automatically created by the FEM2BEM interface to model the crack, and the refinement of the mesh close to the crack tips can be observed. 265 boundary linear elements are used for the local analysis and the computational time is of about 2 minutes.

5.2.2 Global Refined FEM analysis

The Global Refined FEM analysis of a curved cracked stiffened panel results difficult and time expensive. A finest mesh is in fact needed in the region close to the crack (see Fig. 12) with the aim to catch stress concentration at the crack tips. As shown in Fig. 12, the main difficulty associated with the modeling of this kind of structure consists in the transition mesh between the far-crack region and near-crack region, where a refinement is needed. The mesh used for the analysis consists of 40.000 four nodes quadrilateral elements, 200 three nodes triangular elements and 600 bar elements used to model the stringers and the frames. In this case the computing time is about 13 minutes.

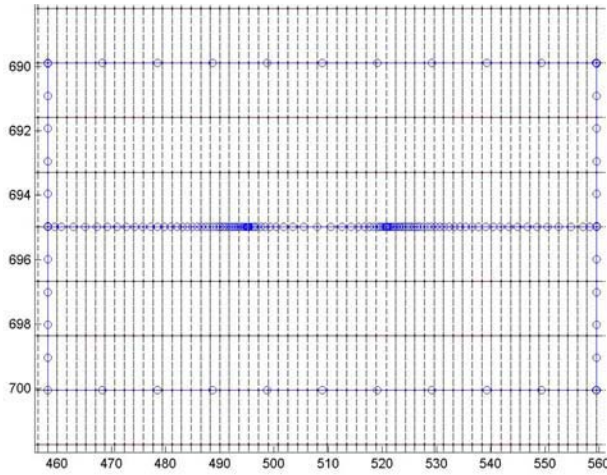


Figure 11: Mesh of the local model.

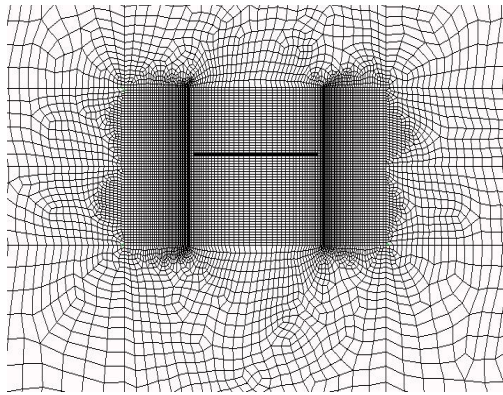


Figure 12: Refined mesh close to the crack.

5.2.3 Comparison and discussions

Fig. 13 shows the Crack Opening Displacements obtained by the present approach and by the Global Refined FEM analysis. A good match can be observed evidencing the accuracy of the Global/Local analysis if compared with the Global Refined FEM ones. This trend is confirmed by the analysis of the stress field close to the crack tips. Fig. 14 shows in fact the circumferential stress distribution close to the crack tip. It can be observed that approaching the singularities the proposed model, and in particular the BEM code used for the local analysis, accurately pre-

dicts the stress distribution if compared with those obtained by the Global Refined FEM analysis. The stress intensity factors characterizing fracture MODE I are also computed directly using the Crack Opening Displacement method (COD). The SIF provided by the two different analyses are $KI=770 \text{ MPa mm}^{1/2}$ by Global/Local and $KI=750 \text{ MPa mm}^{1/2}$ by Global Refined FEM with a percentage differences of 2.6%. Comparing the computational time needed by the two different analysis, great advantages are associates with the use of the proposed Global/Local model. It must also be underlined that the use of the Global/Local approach proposed leads to a substantial reduction of the modeling difficulties and times.

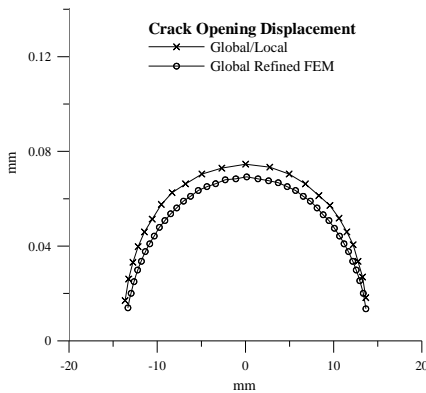


Figure 13: Crack Opening Displacement.

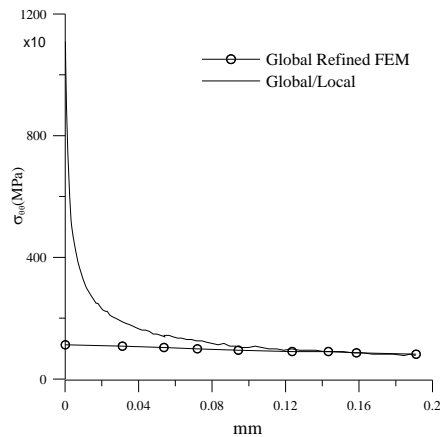


Figure 14: $\sigma_{\theta\theta}$ stress distribution close to the crack tip.

6 Conclusion

In this paper a Global/Local strategy to study the fracture mechanics behavior of complex aerospace structures has been presented. The two different steps of the analysis have been performed by using two different numerical methods. The coarser Global models have been studied by using the finite element code Patran/Nastran™, while a boundary element code for isotropic and anisotropic media, based on a multidomain technique, has been used to analyze the refined local models. An efficient Patran/BEM interface code has been implemented in order to automate the entire procedure. It in fact allows the automatic detection of the cracks and/or holes in a structure and, ones the user has selected the corners of the local region, it allows the automatic creation of the boundary mesh. Great computational efficiency and a substantial reduction of the modeling time have been

achieved by the interface implemented and by the use of the BEM code for the analysis of the local region surrounding the singularity. The model proposed has shown a higher level of accuracy than one would obtain if local refinement is explicitly included in the global mesh. It has been confirmed by the second example proposed, concerning a cracked graphite-epoxy curved panel with Z stiffeners and Z frames.

References

- Noor, A.K.** (2000): *Structure Technology for future Aerospace Systems*, American Institute of Aeronautics and Astronautics.
- Ngo, N.D.; Tamma, K.K.** (2004): An integrated comprehensive approach to the modeling of resin transfer molded composite manufactured net-shaped parts. *CMES: Computer Modeling in Engineering & Sciences*, vol. 5 (2):, pp. 103-133.
- Atluri, S.N.** (1997): *Structural Integrity & Durability*, Tech Science Press.
- Shah, P.D.; Tan, C.L.; Wang, X.** (2006): Evaluation of T-stress for An Interface Crack between Dissimilar Anisotropic Materials Using the Boundary Element Method. *CMES: Computer Modeling in Engineering & Sciences*, vol. 13 (3):, pp. 185-197.
- Forth, S.C.; Staroselsky, A.** (2005): A Hybrid FEM/BEM approach for designing an Aircraft engine Structural Health Monitoring. *CMES: Computer Modeling in Engineering & Sciences*, vol. 9 (3):, pp. 287-298.
- Nikishkov, G.P.; Atluri S.N.** (1994): An analytical-numerical alternating method for elastic-plastic analysis of cracks. *Computational Mechanics*, vol. 3 (6):, pp. 427-442.
- Dornheim, M.A.** (2001): *Low-Fatigue Materials save weight on A380*, Aviation Week & Space Technology.
- King, J.M.C.** (2007): The Airbus 380 and Boeing 787: A role in the recovery of the airline transport market. *Journal of Air Transport Management*, vol. 13, pp. 16-22.
- Mote, C.D.** (1971): Global-Local Finite Element. *International Journal for Numerical Methods in Engineering*, vol. 3, pp. 565-574.
- Zienkiewicz, O.C.; Kelly, D.W.; Bettess, P.** (1997): The coupling of the finite element method and boundary solution procedures. *International Journal for Numerical Methods in Engineering*, vol. 11, pp. 355-375.
- Belyschko, T.; Chang, H.S.; Lu, Y.Y.** (1989): Variationally coupled finite element-boundary element method. *Computers and Structures*, vol. 33, pp. 17-20.
- Belyschko, T.; Fish, J; Bayliss, A.** (1990): The spectral overlay on the finite

element solutions with high gradients. *Computer Methods in Applied Mechanics and Engineering*, vol. 81, pp. 71-89.

Dow, J.; Hardaway J.; Hamernik J. (1992): Combined application of the finite element/finite difference methods. *The 33rd AIAA/ASMEA/ASCE/AHS/ASC Structures, Structural Dynamics and Materials Conference*, Dallas, TX.

Park, J.H.; Singh R.; Pyo C.R.; Atluri S.N. (1995): Integrity of aircraft structural elements with multi-site fatigue damage. *Engineering Fracture Mechanics*, vol. 51(3):, pp. 361-380.

Kawai, H.; Wang, L.; Pipkins, D.S.; O'Sullivan, K.; O'Donoghue, P. E.; Atluri, S.N. (1999): Automation of Global-Intermediate-Local Analysis Based on Feature Based Modelling and the Finite Element Alternating Method. *Computer Modeling and Simulation in Engineering*, vol. 4, pp. 457-464.

Atluri, S.N.; Pipkins, D.S. (1995): Computational strategies for fatigue crack growth in three dimensions with application to aircraft components. *Engineering Fracture Mechanics*, vol. 52 (1):, pp. 51-64.

Pipkins, D.S.; Atluri, S.N. (1996): Applications of the three dimensional finite element alternating method. *Finite Elements in Analysis and Design*, vol. 23, pp. 133-153.

Nikishkov, G.P.; Park, J.K.; Atluri, S.N. (2001): SGBEM-FEM Alternating Method for Analyzing 3D Non-planar Cracks and Their Growth in Structural Components. *CMES: Computer Modeling in Engineering & Sciences*, vol. 2 (3):, pp. 401-422.

Han, Z.D; Atluri, S.N. (2002): SGBEM (for Cracked Local Subdomain)-FEM (for uncracked global Structure) Alternating Method for Analyzing 3D Surface Cracks and their Fatigue-Growth. *CMES: Computer Modeling in Engineering & Sciences*, vol. 3 (6):, pp. 699-716.

Banerjee, P.K.; Butterfield, R. (1981): *Boundary element methods in engineering science*. Mcgraw-Hill, maidenhead.

Blandford, G.E.; Ingraffea, A.R.; Ligget, J.A. (1981): Two-dimensional stress intensity factor computations using boundary element method. *International Journal for Numerical Methods in Engineering*, vol. 17 (3):, pp. 387-404.

Tan, C.L.; Gao, Y.L.; Afagh, F.F. (1992): Boundary element analysis of interface cracks between dissimilar anisotropic materials. *International Journal of Solids and Structures*, vol. 29 (24):, pp. 3201-3220.

Milazzo, A.; Benedetti, I.; Orlando, C. (2006): Boundary Element Method for magneto-electro-elastic laminates. *CMES: Computer Modeling in Engineering & Sciences*, vol. 15 (1):, pp. 17-30.

- MSCSoftware** (2005): *Combined Documentation: MSC.Nastran™, MSC.Patran™*.
- Waszczak, J.P.; Cruse, T.A.** (1971): Failure mode and strength prediction of anisotropic bolt bearing specimens. *Journal of Composite Materials*, vol. 5, pp. 421-425.
- DeJong, T.** (1977): Stress around pin loaded hoers in elastically orthotropic or isotropic plates. *Journal of Composite Materials*, vol. 11, pp. 313-331.
- Her, S.C.; Shie D.L.** (1998): The failure analysis of bolted repair on composite laminate. *International journal of solids and structures*, vol. 35 (15);, pp. 1679-1693.
- Davì, G.; Milazzo, A.** (2001): Multidomain boundary integral formulation for piezoelectric materials fracture mechanics. *International Journal of Solids and Structures*, vol. 38, pp. 7065-7078.
- Davì, G.** (1989): A general boundary formulation for the numerical solution of bending multilayer sandwich plates. In: Brebbia, C.A. Connor, J.J. (Eds.), *Advances in Boundary Elements. Proceedings of the 11th International Conference on Boundary Element Methods*. Computational Mechanics Publications, Southampton, pp. 25-35.
- Lekhnitskii, S.G.** (1963): *Theory of elasticity of an anisotropic body*, Holden-Day, San Francisco.
- Aliabadi, M.H.** (2002): *The boundary element method, volume 2 applications in solids and structures*, John Wiley & Sons, LTD.
- Armentani E.; Citarella, R.** (2006): DBEM and fem analysis on non-linear multiple crack propagation in an aeronautic doubler-skin assembly. *International Journal of Fatigue*, vol. 28, pp. 598-608.
- AGARD-CP-427** (1987): *Behavior and analysis of mechanically fastened joints in composite structures*, AGARD-CP-427.
- Young, R.D.; Rose, C.A.; Starnes Jr, J.H.;** (2001): *Skin, stringer, and fastener loads in buckled fuselage panels*, AIAA, 1326.

